AGU PUBLICATIONS

Geophysical Research Letters

RESEARCH LETTER
10.1002/2017GL075745

Key Points:
- Using a synchronously coupled ice sheet/ice shelf/ocean model, ice sheet response to climate variability is assessed
- Oscillations in thermocline depth at varying periods induce a nonlinear response in the amplitude of change in grounded ice
- The nonlinear response highlights the heightened sensitivity of fast flowing ice streams to climate variability on the decadal time scales

Supporting Information:
- Supporting Information S1

Correspondence to:
D. N. Goldberg,
dngoldberg@gmail.com

Citation:
Snow, K., Goldberg, D. N., Holland, P. R., Jordan, J. R., Arthern, R. J., & Jenkins, A. (2017). The response of ice sheets to climate variability. *Geophysical Research Letters*, *44*, 11,878–11,885. https://doi.org/10.1002/2017GL075745

Received 22 SEP 2017
Accepted 6 NOV 2017
Published online 11 DEC 2017

The Response of Ice Sheets to Climate Variability

K. Snow[1], D. N. Goldberg[1], P. R. Holland[2], J. R. Jordan[2], R. J. Arthern[2], and A. Jenkins[2]

[1]School of Geosciences, University of Edinburgh, Edinburgh, UK, [2]British Antarctic Survey, Cambridge, UK

Abstract West Antarctic Ice Sheet loss is a significant contributor to sea level rise. While the ice loss is thought to be triggered by fluctuations in oceanic heat at the ice shelf bases, ice sheet response to ocean variability remains poorly understood. Using a synchronously coupled ice-ocean model permitting grounding line migration, this study evaluates the response of an ice sheet to periodic variations in ocean forcing. Resulting oscillations in grounded ice volume amplitude is shown to grow as a nonlinear function of ocean forcing period. This implies that slower oscillations in climatic forcing are disproportionately important to ice sheets. The ice shelf residence time offers a critical time scale, above which the ice response amplitude is a linear function of ocean forcing period and below which it is quadratic. These results highlight the sensitivity of West Antarctic ice streams to perturbations in heat fluxes occurring at decadal time scales.

1. Introduction

The West Antarctic Ice Sheet's contribution to global sea level rise has increased dramatically in recent decades, with the ice mass loss doubling from 2003 to 2014 (Harig & Simons, 2015; Shepherd et al., 2012). A strong trigger for the recent change is thought to be a variability in the oceanic heat fluxes delivered to ice shelf bases (Dutrieux et al., 2014; Jenkins et al., 2016). This oceanic variability has been linked to the El Niño–Southern Oscillation (ENSO) (Ding et al., 2011; Dutrieux et al., 2014; Steig et al., 2012). The ENSO teleconnections between the tropical Pacific and a low-pressure system over the South Pacific (the Amundsen Sea Low) (Ding et al., 2011; Simmonds & King, 2004) mean that the West Antarctic region experiences some of the strongest signals of interannual to decadal scale variability within the Southern Hemisphere (Jenkins et al., 2016).

It has been suggested that the current retreat of Pine Island Glacier (PIG) in the Amundsen Sea may be linked to climate anomalies occurring during El Niño events in the 1940s and 1970s (Smith et al., 2017). El Niño events lead to a shallowing of the thermocline and relatively warm ocean conditions in the Amundsen Sea (Ding et al., 2011; Dutrieux et al., 2014; Steig et al., 2012), triggering enhanced melt and possible retreat. During the La Niña period of 2012, summer thermocline depths in front of Pine Island Glacier (PIG) deepened by about 250 m compared to previously observed years.

Despite the proposed links between climate variability and ice sheet change, our understanding of the sensitivity of ice sheets to variable ocean forcing remains poor. This is largely a result of limited observations in the extreme Antarctic region and the early stage of development of coupled ice sheet–ocean models. Most coupled models separately evolve the ice sheet and ocean components in a discontinuous or asynchronous manner, leading to potential problems with the neglect of ocean history or with nonconservation of heat and volume in the ocean model. In this context, we refer to "discontinuous" as coupling in which an entirely new ocean model is initialized every ice model time step, and "asynchronous" as coupling in which there is simultaneous progression of the ice and ocean models and information is exchanged at the ice time step, following the terminology of Jordan et al. (2017). In this study, we apply a novel method of synchronous ice-ocean coupling that evolves the ice sheet and ocean simultaneously within a single model code (Jordan et al., 2017). This model may be particularly appropriate for considering rapidly varying oceanic forcing of ice sheets, where ocean history and accurate conservation could be important.

While fully coupled models are necessary to provide a complete account of the ice-ocean response to climate variability, some insight has been obtained from dynamically simplified and uncoupled studies (e.g., Aykutlug & Dupont, 2015; Tsai & Gudmundsson, 2015; Williams et al., 2012). Williams et al. (2012) investigate the

upstream propagation of changes in grounding-line strain rates within an idealized ice stream model. They find two distinct regimes of upstream propagation dependent on the frequency of variation in their forcing. At low frequencies (centennial), changes occur through adjustment of the grounding line and ice geometry. At high frequencies (annual to decadal), ice geometry varies little while the velocities adjust rapidly, propagating changes upstream via membrane stresses. How ocean variability additionally influences the amplitude of the strain rates at the grounding line was not considered in their study.

Holland (2017) considers the transient response of ice shelf melting to variable ocean forcing. For ocean oscillations slower than the ocean cavity residence time, melting anomalies adhere to the equilibrium response derived from steady simulations and transient ocean history is unimportant. In our simulations, forcing periods are significantly greater than the ocean cavity residence time (≈3 months), so we expect melt rates to be in equilibrium with ocean forcing conditions.

In this study, we consider the response of a coupled ice sheet-ocean model to oscillating ocean forcing conditions. Our primary aim is to assess how the amplitude of the grounded ice response varies as a function of the period of the oscillating ocean forcing—the *frequency response*. This will provide crucial insight into which time scales of ocean and climate variability are most important to West Antarctic ice streams.

An idealized ice-ocean configuration is defined (section 2) to provide a simple means of diagnosing how oscillations in ocean thermocline depth influence ice sheet characteristics for a variety of oscillation periods. The coupled results are complemented with longer uncoupled ice-only runs, adopting a novel melt parameterization calibrated by the coupled model. The results (section 3) show a nonlinear relationship between the amplitude of ice sheet mass fluctuations and the ocean forcing oscillation period, as well as a change in time mean ice sheet mass despite zero-time mean forcing. Such nonlinearities support the evidence that extreme events triggered by variable climate conditions, such as ENSO, may drive enhanced adjustments of the West Antarctic Ice Sheet.

2. Method

2.1. Synchronous Coupling

The model framework for all experiments is based within the Massachusetts Institute of Technology General Circulation Model (MITgcm; Marshall et al., 1997). Synchronous coupling occurs between the ocean component of MITgcm and a hybrid stress balance ice stream model (Goldberg & Heimbach, 2013). Thickening and thinning of the water column every time step through ocean adjustment to ice shelf dynamics and melt occurs through a vertical coupling method described in detail by Jordan et al. (2017). The vertical coupling includes adjusting the ocean/ice mask in the ocean model to account for changes in the size of the ocean domain. We permit such adjustment to occur on a "remeshing" frequency (Jordan et al., 2017) of 5 days.

To additionally permit grounding line retreat/advance, water needs to be transferred horizontally in a method analogous to wetting/drying. Transferring water horizontally to a previously "dry" water column, however, is difficult in primitive equation ocean models such as MITgcm due to the implicit formulation of the free surface equation (Campin et al., 2004), which is necessary for efficient model performance. Hence, we have chosen to retain the implicit free surface by enforcing the existence of a thin ocean layer everywhere beneath grounded ice. The layer is defined by a maximum surface pressure field and is on average 6 m thick (maximum 8 m), is restored to initial tracer conditions and zero velocities, and does not interact thermodynamically with the ice. The thicknesses ensure that the subglacial layer remains horizontally continuous across the step-like bathymetry in the MITgcm's Cartesian coordinates. As surface pressures adjust upon grounding line retreat or advance, the expansion or contraction of the ice shelf cavity waters are thus permitted as the subglacial layer region adjusts (section S1 in the supporting information).

2.2. Model Characteristics

In the coupled framework, an idealized ice-ocean domain is defined (Figure 1a) with 20 m vertical and 1 km horizontal resolution. Bathymetry with a reverse slope of 0.001 is prescribed under the ice, tapering to a flat bed under the open ocean. An ice influx of 2×10^5 m^2 a^{-1} per unit width is prescribed at the "southern" boundary with a fixed calving front at 300 km, and no-slip conditions at the "east"-"west" boundaries. The "northern" ocean boundary is restored to temperature and salinity profiles representative of conditions observed in the Amundsen Sea (Figure 1b, De Rydt et al., 2014; Holland, 2017). The boundary restoring occurs over a width of 10 km with a time scale increasing linearly from 1 day to 10 days on the inner edge. Side wall ocean boundaries are free slip, and a quadratic ocean bottom drag coefficient of 2.5×10^{-3} is used.

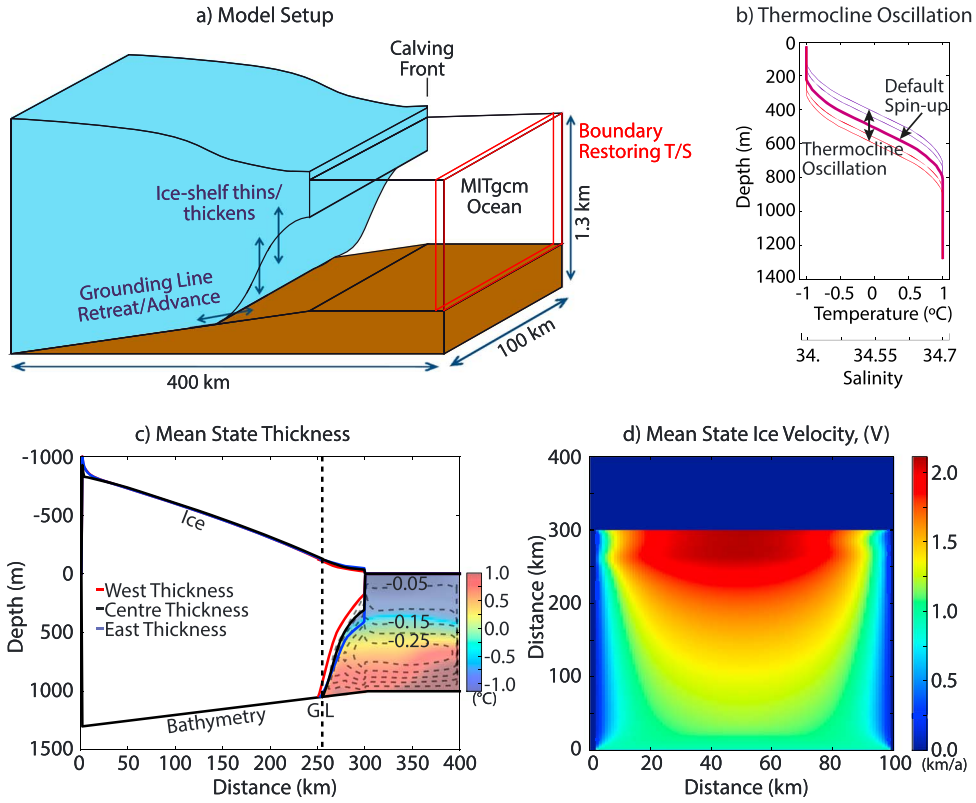

Figure 1. (a) Schematic of the coupled model setup including the ice and ocean domains. (b) Temperature (°C) and salinity profiles versus depth (m) used in the restoring boundary condition of the ocean. The thick line represents the mean state used in spin-up, while the blue and red lines indicate the range of profiles used in the periodic oscillations of the thermocline. (c) Resulting spun-up ice thicknesses at the center (black) and 5 km from the eastern (blue) and western (red) boundaries, respectively, along with center grounding line (GL) location (black dashed line). Filled contours show the temperature profile in the center of the domain, and grey dashed lines are the longitudinally averaged meridional overturning stream function with 0.05 Sv spacing. (d) Resulting spun-up ice velocity (km a^{-1}).

Melting occurs at the ice-ocean interface using the "three-equation" approach with parameters calibrated from Jenkins et al. (2010): quadratic drag coefficient is $C_d = 0.0097$ and turbulent heat and salt exchange coefficients are $\Gamma_T = 0.011$ and $\Gamma_S = 0.00031$, respectively. In the ice model, Weertman-style basal friction is applied (basal friction coefficient of 1600 Pa $(m/a)^{-1/3}$) and ice rheology is described by a Glen's flow law with exponent $n = 3$ and fluidity constant $A = 2.7 \times 10^{-25}$ $Pa^{-3}s$ (corresponding to a uniform ice temperature of −14.7°C). For further details of model parameter settings see Table S1.

2.3. Coupled Perturbation Experiments

The model is initially spun-up applying the average temperature and salinity profiles (bold lines in Figure 1b; section S1 in the supporting information). At the end of the spin-up, the mean and monthly standard deviation of the bulk melt and volume above floatation (VAF) in the final decade of spin-up were (124.2 ± 0.2) Gt a^{-1} and 9196.9 ± 0.5 km^3, respectively. VAF is the volume of ice that could contribute to sea level rise and is often used as an indicator of adjustment of grounded ice.

Once the coupled model is spun-up to the state described above, the temperature and salinity profiles restored at the northern boundary are varied in time. The thermocline center is oscillated between 400 m and 600 m (representative of observed Amundsen Sea variability; De Rydt et al., 2014; Dutrieux et al., 2014) using a closed cycle of given period, with each period being supplied with 100 profiles varying temperature and salinity (T/S) in a sinusoidal manner (and linearly interpolated in between; Figure 1b). The defined periods of thermocline depth oscillation are 2, 5, 10, 15, 20, 25, 30, and 50 years, with monthly mean results output. Longer periods are not possible in the current configuration due to the computational expense of running the coupled model on centennial time scales. Hence, to supplement the coupled runs, a series of ice-only runs with parameterized melt rate are also undertaken.

2.4. Uncoupled Ice-Only Perturbation Experiments

The ice-only runs use the same bathymetry and ice initial conditions as the coupled runs. We derive the melt parameterization representing varying thermocline depth by considering the range of melt profiles spanning a complete oscillation period in the coupled runs. Using the 2 year forcing with output after 30 years of repeat oscillations, we plot the melt profiles against depth (Figure 2a; grey points) and calculate the linear profiles of the two extreme states within the depth range from 300 to 800 m (dashed lines; Figure 2a). Melt above 300 m is set to zero and melt below 800 m is fixed to that derived at 800 m (black line Figure 2b). The melt is then oscillated between the two linear profiles in a sinusoidal manner over the given period (grey lines; Figure 2b). Melt profiles for other coupled periods illustrated similar characteristics to the 2 year case (not shown), so we use the coupled 2 year run to derive the melt profile for all uncoupled periods.

In addition to the depth-dependent characteristics, an additional criterion is applied in which melt decreases linearly to zero within 10 km of the grounding line (e.g., 2 km from the grounding line, it is $\frac{1}{5}$ times the depth-dependent value). This latter criterion is an attempt to recreate the tapering off of melt rates seen in the coupled runs near the grounding line (Figure 2d). Note, our aim here is merely to obtain a parameterization that accurately reflects the coupled model results, not to generate a parameterization that is generally representative of ice shelf melt rates.

The result of the above parameterization, defined as the symmetric uncoupled (Sym) run, reproduces the broad scale characteristics of the coupled mean melt field (Figures 2d and 2e). The most noticeable difference is the lack of east-west variation, with high melting on the Coriolis-favored side in the coupled runs. Hence, a second set of parameterized melt runs are also implemented, defined as the asymmetric uncoupled (Asym) runs, in which the Sym profile is scaled linearly from east to west using a multiple of 0.66 to 1.33 (Figure 2c). The latter melt profile is thus able to capture the broad scale features of the coupled melt (Figure 2f).

A final uncoupled run, referred to as the slow uncoupled case, is also undertaken following the same setup as the symmetric uncoupled case but with a slower southern boundary ice influx of 1.5×10^5 m^2 a^{-1} per unit width and basal friction coefficient of 50 Pa (m/a)$^{-1/3}$. To achieve an ice equilibrium state with less ice influx while maintaining the parameterization characteristics, the imposed melt is also halved compared to the symmetric uncoupled case.

The oscillation periods covered in the uncoupled runs include every 2.5 years from 2.5 to 30 years, and then every decade up to 100 years. In each case the ice has been spun-up (run for 1,000 years) with the mean parameterized melt profile and the oscillations then initiated and continued for 600 years. Time-averaged results are output every month for the 2.5 year case, every 3 months for periods less than 15 years and every year for longer periods.

3. Results

3.1. Mean States

3.1.1. Coupled Spun-up State

Before moving to the results of the variable forcing response, we first provide details of the coupled spun-up state. The mean melt rate shows strong enhancement on the Coriolis favored side of the domain (Figure 2d), and leads to a shelf averaged melt rate of 25.7 m a^{-1}. The spatial variability of melt causes transverse variation in ice thickness, with the thickest ice shelf occurring in the east (Figure 1c). The resultant ice velocity has a peak at the grounding line reaching a maximum of 2,113 m a^{-1}. The spun up ocean reveals an overturning stream function of approximately 0.25 Sv (Figure 1c). Ocean temperatures range from 1 to −1.3°C and salinity (not shown) increases with depth up to 34.7.

3.1.2. Variable Forcing: Long-Term Drift

On applying the variable forcing in ocean thermocline depth to the spun-up model, both periodic variability and a long-term drift (or rectification) in VAF are found (Figures 2j–2l). The presence of the drift is thought to arise from the depth dependence of the melt rate (section S3.1 in the supporting information); however, what determines positive drift (advance) over negative drift (retreat) is not fully understood (section S3.2 in the supporting information). The spatial distribution of the melt seems to play a key role given the alternative trend in VAF for the "Sym" and "Asym" cases, the latter yielding a qualitatively similar drift response to the coupled runs. Similar conclusions were obtained from Gagliardini et al. (2010), who found that an increase in melt may in fact induce ice sheet advance depending on how the melt increase is distributed and how it

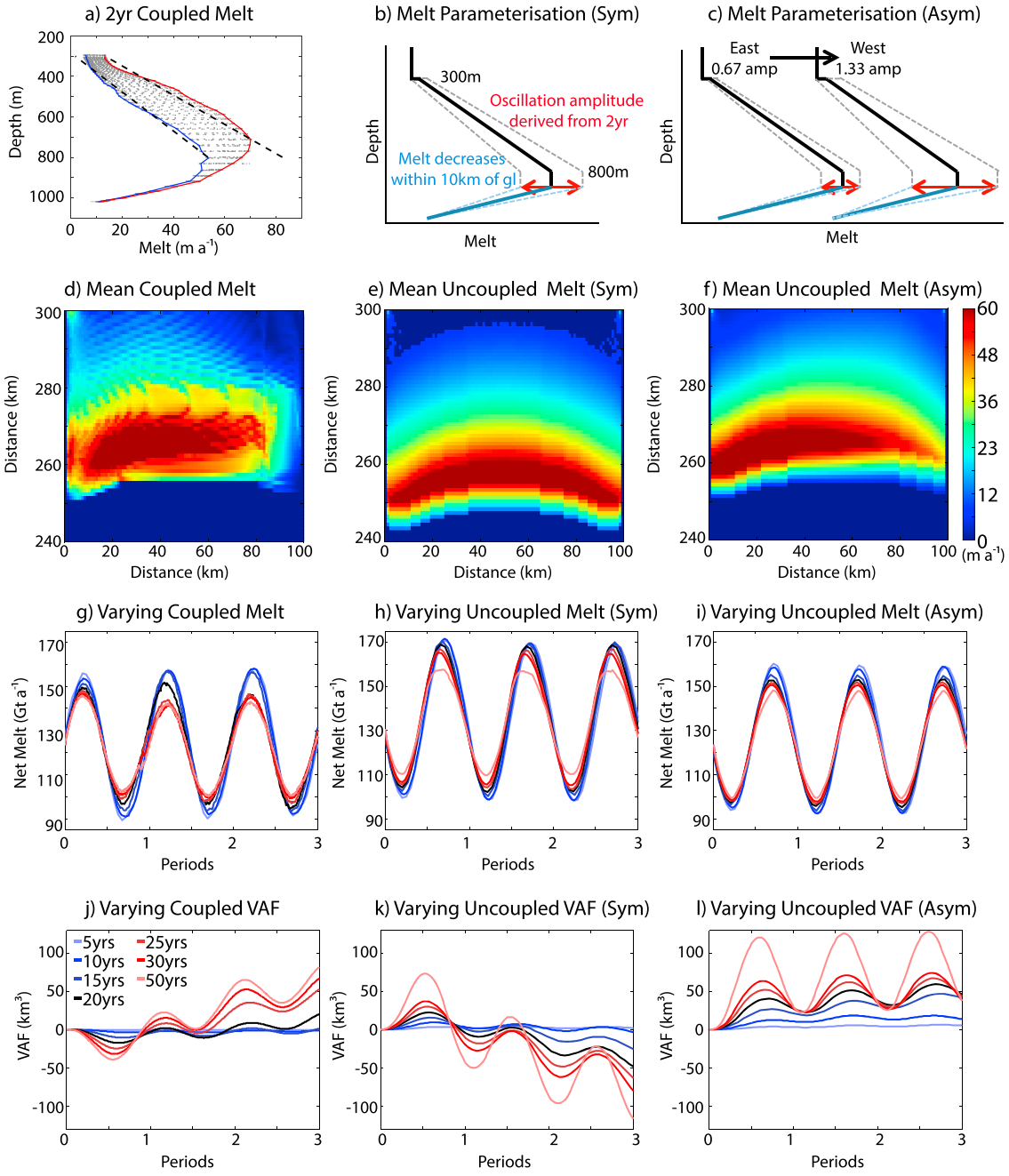

Figure 2. (a) Monthly mean melt (m a^{-1}) rates versus depth (m) over the final period of the 2 year coupled run (grey points). The maximum and minimum profiles are given by the red and blue lines, respectively, and the linear trend of those profiles between 300 and 800 m given by the dashed lines. Derived schematic representation of the parameterized melt profile and how it is oscillated are indicated for the (b) symmetric and (c) asymmetric cases and the resultant spatial variation of the mean ice shelf melt in the (d) coupled, (e) symmetric uncoupled, and (f) asymmetric uncoupled cases. Time series of bulk melt (Gt a^{-1}) and VAF anomaly from initial state (km^3: initial VAF is 9,198, 8,685 and, 11,262 km^3 for Figures 2j–2l, respectively) versus time normalized by oscillation period in the (g, j) coupled, (h, k) symmetric uncoupled, and (i, l) asymmetric uncoupled runs, respectively, for periods of 5–50 years.

influences lateral resistance of the ice. The complexity of the ice response in relation to the melt characteristics, if anything, further emphasizes the importance of having the coupled model to provide the details of the spatiotemporal melt distribution.

With this paper being focused on the variable response of the ice, rather than the long-term drift, the remainder of our analysis investigates the relationship between the period of ocean forcing oscillations and the amplitude of ice response to oscillations. The amplitude of response indicates how different modes and

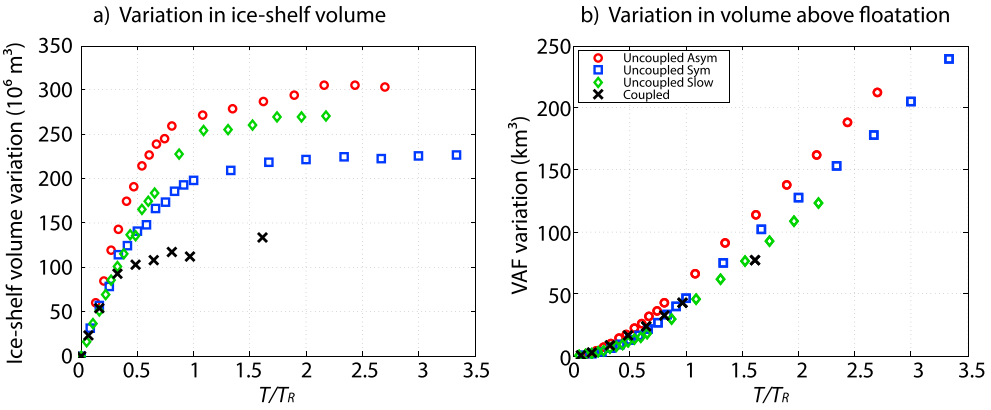

Figure 3. (a) Mean variation in ice shelf volume (10^6 m^3) and (b) VAF (km^3) versus period normalized by ice shelf residence time (T/T_R) for the uncoupled symmetric (blue squares), asymmetric (red circles), slow (green diamonds), and coupled (black crosses) cases.

timescales of climate variability may have triggered an adjustment in the West Antarctic Ice Sheet (e.g., ENSO; see section 1). Subsequent results of such variability are derived from the time series of the de-trended (removal of the long-term drift) states.

3.2. Variability Response

3.2.1. Melt Variation

Time series of bulk melt indicate the range of variability induced by periodic oscillations in thermocline depth (Figures 2g–2i). A trend of decreasing variability with increasing period results from the depth dependence of melting and the thinning/thickening response time of the ice shelf. If the thermocline is shallowed, the melt will increase, but if the ice shelf has enough time to respond by thinning (decreasing the area of deep high melt), the magnitude of this melt increase will be damped. Thus, the decreasing amplitude of melt variation with increasing ocean forcing period is indicative of the ice's capacity to adjust over time to the new melt conditions.

3.2.2. Nonlinear Ice Shelf Volume Response

The decrease in melt amplitude with increasing forcing period indicates the ability of the ice shelf to approach an unsteady "cyclic quasi-equilibrium" state, in which the ice shelf is fully adjusted to the forcing at all stages of the forcing cycle. (Note, it is not a true cyclic equilibrium, because the ice sheet adjusts on even slower time scales, taking centuries to fully adjust to a step change in thermocline depth and change in buttressing).

The quasi-equilibrium can be seen by considering the amplitude of ice shelf volume oscillations as a function of the period of ocean forcing oscillations (Figure 3a). It is informative to normalize the forcing period T by the ice shelf residence time T_R. Ice shelf residence times are 31, 37, 30, and 46 years for the coupled and uncoupled symmetric, asymmetric, and slow cases, respectively. The amplitude of ice volume variations is derived from a detrended time series, in which a moving average with window width equal to the oscillation period is removed from the original time series. In this way we focus on the characteristics of the variability rather than long-term drift.

Two distinct regimes exist in the variability of ice shelf volume with forcing period T, with the approximate transition point being near the ice shelf residence time, T_R:

1. For $T < T_R$: variation in shelf volume is *proportional* to T.
2. For $T > T_R$: variation in shelf volume is *constant* with T.

The change in characteristics of the ice shelf volume variation with forcing period is a result of the cyclic quasi-equilibrium state that the ice shelf may achieve for "slowly varying" forcing. For longer forcing oscillation periods, the ice will be adjusted to the thermocline depth at all times, meaning that the minimum and maximum ice shelf volume depend only on the maximum and minimum thermocline depth—and not on the forcing time scale. On the other hand, for "rapidly varying" forcings, the ice shelf geometry will not be in balance with the instantaneous forcing. In this regime, the amplitude of ice volume oscillations grows with forcing oscillation period because the amount of ice removed by a given melt anomaly is proportional to both

the rate of melting and the duration over which the anomaly persists. Our simulations show that the transition between rapidly varying and slowly varying behaviors occurs near the time scale of the ice shelf residence time, T_R.

3.2.3. Nonlinear Change in VAF With Period

Ice shelf volume plays a significant role in controlling the buttressing of ice sheets, so it is natural to assume that the rate of change of VAF is proportional to the anomaly in ice shelf volume. A smaller ice shelf offers less back stress, instantaneously permitting faster flow, which then progressively draws down grounded ice (see also section S4 in the supporting information). The amplitude of VAF oscillations is thus proportional to the amplitude of ice shelf volume oscillations, multiplied by forcing period:

1. For $T < T_R$: VAF variation is proportional to T^2.
2. For $T > T_R$: VAF variation is proportional to T.

This result is borne out by the simulations (Figure 3b). For slowly varying forcing, the ice shelf volume oscillation amplitude remains fixed as the forcing period gets longer, but shelf volume anomalies persist for longer, so VAF oscillation amplitude increases with the forcing period. For rapidly varying forcing, both the ice shelf volume oscillation amplitude and the persistence of ice shelf volume anomalies increase with the forcing period, and VAF oscillation amplitude increases as the forcing period squared.

The importance of the residence time is demonstrated by considering the "uncoupled slow" simulation, in which T_R is 46 years. When the forcing periods are not normalized by residence time (supporting information Figure S8), the "slow" result does not collapse onto the others as in Figure 3b. To further demonstrate the nonlinear characteristics of our results, curve-fitting techniques are applied to the results in Figure 3b. Continuous linear, continuous quadratic, and a piecewise quadratic to linear functions are all fit to the data (section S6). In all uncoupled cases the sum of the squared errors is smallest and the adjusted R squared value greatest for the piecewise nonlinear solution (R^2 averaging 0.9995; Table S2), while in the coupled case the quadratic solution fits best (there are not enough points in the linear section to produce a suitable piecewise nonlinear fit). The transition from quadratic to linear is also found to occur on average at $T/T_R = 1.01$ and thus presents further validation that in our simulations the turning point of the quadratic to linear solution of VAF amplitude occurs at the ice shelf residence time.

4. Discussion

4.1. Implications of Synchronous Coupling

A new synchronous approach to ice sheet-ice shelf-ocean coupling was used in this study, and it is worth considering whether the behavior observed hinges on this as this has implications for future coupled modeling studies. While we emphasize the importance of providing correct spatiotemporal distributions of the melt rate in order to achieve the rectified response, it is conceivable that our results could have been achieved through asynchronous means. Indeed, the key mechanism involved in the frequency response—the adjustment of the ice shelf to new ocean conditions on the residence time scale—has been observed in asynchronous/discontinuous coupled studies (Goldberg et al., 2012). We believe our method has unique advantages through being able to represent the spectrum of time scales coupling the ice and the ocean, while at the same time not sacrificing computational expense relative to any asynchronous approach which takes account of ocean history. However, further work is needed to fully understand the implications of the different methods in different scenarios.

4.2. Implications of Ice Shelf Residence Time

Pine Island Glacier (PIG) ice shelf, 80 km long and flowing at 4 km a^{-1}, has a residence time of the order of 20 years. The nonlinear characteristics of the VAF variation with period means that PIG will exhibit increased sensitivity to periodic forcing approaching decadal time scales. It is possible that the interannual- to decadal-scale periodic forcing of ENSO (e.g., Stuecker et al., 2013), hypothesized to have led to the current potentially unstable retreat of PIG, did not occur only through the extreme conditions present during the 1940s El Niño (Smith et al., 2017) but also through the heightened sensitivity of the ice sheet to longer-term modes of variability. While it is beyond the scope of this study to investigate this specific linkage more closely, further work is underway to investigate the dominant modes of climate variability in West Antarctica and the potential role of nonlinearities in VAF response.

5. Summary and Conclusion

West Antarctic ice shelves are exposed to some of the warmest deep waters available on the entire Antarctic continental shelf. Variation in the inflow of these waters (hence local thermocline depths) are intimately linked to interannual and decadal modes of climate variability (Ding et al., 2011; Dutrieux et al., 2014; Jenkins et al., 2016; Steig et al., 2012). The subsequent fluctuations in heat delivered to the base of the ice shelves have the potential to trigger ice instability and drive large-scale change (Smith et al., 2017) leading to sea level rise (e.g., Harig & Simons, 2015). Improving our understanding of the sensitivity of ice sheets to ocean variability is thus paramount in assessing the potential impacts of future climate change.

A series of coupled ice sheet/ice shelf/ocean simulations are undertaken to investigate ice sheet sensitivity to periodic oscillations in thermocline depth, emulating observed variability in front of West Antarctic ice shelves. The coupled runs are complemented by a series of ice-only runs, implementing novel melt parameterizations calibrated by the coupled model. Simulations with a range of forcing periods reveal two response regimes, delineated by the ice shelf residence time. For forcing periods less than the residence time, the amplitude of change in ice sheet volume above floatation (VAF) is a quadratic function of ocean forcing period, while for longer periods a linear relationship holds.

The nonlinear change in VAF with variations in thermocline depth at periods less than the residence time indicates the reduced sensitivity of ice sheets to faster climate modes. A near fourfold increase in VAF variation with only a doubling of the period from 5 to 10 years is found for an ice shelf of residence time 31 years. This heightened sensitivity of the VAF to interannual- and decadal-scale variability may play an important role in defining West Antarctica's response to climatic changes. To determine the full VAF response to climate variability, the VAF amplitude-forcing period relationship determined here would need to be convolved with the power spectrum of the climate forcing signal. Our results demonstrate that the ice-ocean system will amplify any longer-period variability present in that signal.

Acknowledgments
This work was supported by Natural Environment Resources Council grant NE/M003590/1. The code used to generate all results is available freely at mitgcm.org. The model output used to generate Figures 2, 3, and S3–S8 is available for download at https://doi.org/cgb9.

References

Aykutlug, E., & Dupont, T. K. (2015). A sensitivity study of fast outlet glaciers to short timescale cyclical perturbations. *The Cryosphere Discussions*, *9*, 223–250.
Campin, J., Adcroft, A., Hill, C., & Marshall, J. (2004). Conservation of properties in a free-surface model. *Ocean Modelling*, *6*, 221–244.
De Rydt, J., Holland, P. R., Dutrieux, P., & Jenkins, A. (2014). Geometric and oceanographic controls on melting beneath Pine Island glacier. *Journal of Geophysical Research: Oceans*, *119*, 2420–2438. https://doi.org/10.1002/2013JC009513
Ding, Q., Steig, E. J., Battisti, D. S., & Küttel, M. (2011). Winter warming in West Antarctica caused by central tropical Pacific warming. *Nature Geoscience*, *4*, 398–403.
Dutrieux, P., De Rydt, J., Jenkins, A., Holland, P. R., Ha, H. K., Lee, S. H., … Schröder, M. (2014). Strong sensitivity of Pine Island ice-shelf melting to climate variability. *Science*, *343*, 174–178.
Gagliardini, O., Durand, G., Zwinger, T., Hindmarsh, R. C. A., & Le Meur, E. (2010). Coupling of ice-shelf melting and buttressing is a key process in ice-sheet dynamics. *Geophysical Research Letters*, *37*, L14501. https://doi.org/0.1029/2010GL043334
Goldberg, D. N., & Heimbach, P. (2013). Parameter and state estimation with a time-dependent adjoint marine ice sheet model. *The Cryosphere*, *7*, 1659–1678.
Goldberg, D. N., Little, C. M., Sergienko, O., Gnanadesikan, A., Hallberg, R., & Oppenheimer, M. (2012). Investigation of land ice-ocean interaction with a fully coupled ice-ocean model: 1. Model description and behavior. *Journal of Geophysical Research*, *117*, F02037. https://doi.org/10.1029/2011JF002246
Harig, C., & Simons, F. J. (2015). Accelerated West Antarctic ice mass loss continues to outpace East Antarctic gains. *Earth and Planetary Science Letters*, *415*, 131–141.
Holland, P. (2017). The transient response of ice-shelf melting to ocean change. *Journal of Physical Oceanography*, *47*, 2102–2114.
Jenkins, A., Nicholls, A. K. W., & Corr, H. F. J. (2010). Observation and parameterization of ablation at the base of Ronne Ice Shelf. *Journal of Physical Oceanography*, *40*, 2298–2312.
Jenkins, A., Dutrieux, P., Jacobs, S., Steig, E., Gudmundsson, G., Smith, J., & Heywood, K. (2016). Decadal ocean forcing and Antarctic ice sheet response: Lessons from the Amundsen Sea. *Oceanography*, *29*, 106–117.
Jordan, J. R., Holland, P. R., Goldberg, D., Snow, K., Arthern, R., Heimbach, P., … Jenkins, A. (2017). Ocean-forced ice-shelf thinning in a synchronously coupled ice-ocean model. *Journal of Geophysical Research: Oceans*, *122*. https://doi.org/10.1002/2017JC013251
Marshall, J., Hill, C., Perelman, L., & Adcroft, A. (1997). Hydrostatic, quasi-hydrostatic, and nonhydrostatic ocean modeling. *Journal of Geophysical Research*, *102*, 5733–5752.
Shepherd, A., Ivins, E. R., Gerou, A., Barletta, V. R., Bentley, M. J., Bettadpur, S., … Zwally, H. J. (2012). A reconciled estimate of ice-sheet mass balance. *Science*, *338*, 1183–1189.
Simmonds, I., & King, J. C. (2004). Global and hemispheric climate variations affecting the Southern Ocean. *Antarctic Science*, *4*, 401–413.
Smith, J. A., Andersen, T. J., Shortt, M., Gaffney, A. M., Truffer, M., Stanton, T. P., … Vaughan, D. G. (2017). Sub-ice-shelf sediments record history of twentieth-century retreat of Pine Island Glacier. *Nature*, *541*, 77–80.
Steig, E. J., Ding, Q., Battisti, D. S., & Jenkins, A. (2012). Tropical forcing of circumpolar deep water inflow and outlet glacier thinning in the Amundsen Sea embayment, West Antarctica. *Annals of Glaciology*, *53*, 19–28.
Stuecker, M. F., Timmermann, A., Jin, F., McGregor, S., & Ren, H. (2013). A combination mode of the annual cycle and the El Niño/Southern Oscillation. *Nature Geoscience*, *6*, 540–544.
Tsai, V. C., & Gudmundsson, G. H. (2015). An improved model for tidally modulated grounding-line migration. *Journal of Glaciology*, *61*, 216–222.
Williams, C. R., Hindmarsh, R. C. A., & Arthern, R. J. (2012). Frequency response of ice streams. *Proceedings of the Royal Society A*, *468*, 3285–3310.